AJNR

Imaging of Cauda Equina Edema in Lumbar Canal Stenosis By Using Gadolinium-Enhanced MR Imaging: Experimental Constriction Injury

S. Kobayashi, K. Uchida, K. Takeno, H. Baba, Y. Suzuki, K. Hayakawa and H. Yoshizawa

AJNR Am J Neuroradiol 2006, 27 (2) 346-353
http://www.ajnr.org/content/27/2/346

ORIGINAL RESEARCH

Imaging of Cauda Equina Edema in Lumbar Canal Stenosis By Using Gadolinium-Enhanced MR Imaging: Experimental Constriction Injury

S. Kobayashi
K. Uchida
K. Takeno
H. Baba
Y. Suzuki
K. Hayakawa
H. Yoshizawa

BACKGROUND AND PURPOSE: It has been reported that disturbance of blood flow arising from circumferential compression of the cauda equina by surrounding tissue plays a major role in the appearance of neurogenic intermittent claudication (NIC) associated with lumbar spinal canal stenosis (LSCS). We created a model of LSCS to clarify the mechanism of enhancement within the cauda equina on gadolinium-enhanced MR images from patients with LSCS.

METHODS: In 20 dogs, a lumbar laminectomy was performed by applying circumferential constriction to the cauda equina by using a silicon tube, to produce 30% stenosis of the circumferential diameter of the dural tube. After 1 and 3 weeks, gadolinium and Evans blue albumin were injected intravenously at the same time. The sections were used to investigate the status of the blood-nerve barrier function under a fluorescence microscope and we compared gadolinium-enhanced MR images with Evans blue albumin distribution in the nerve. The other sections were used for light and transmission electron microscopic study.

RESULTS: In this model, histologic examination showed congestion and dilation in many of the intraradicular veins, as well as inflammatory cell infiltration. The intraradicular edema caused by venous congestion and Wallerian degeneration can also occur at sites that are not subject to mechanical compression. Enhanced MR imaging showed enhancement of the cauda equina at the stenosed region, demonstrating the presence of edema.

CONCLUSION: Gadolinium-enhanced MR imaging may be a useful tool for the diagnosis of microcirculatory disorders of the cauda equina associated with LSCS.

Lumbar spinal canal stenosis (LSCS) is increasingly a common disease in the elderly. The number of patients with LSCS complaining of low back pain, lower extremity pain and/or numbness, and neurogenic intermittent claudication (NIC) has increased yearly.[1,2] Whether mechanical deformation or a circulatory disturbance plays the more prominent role in the pathogenesis of NIC with LSCS has been a subject of speculation for more than 5 decades. In 1954, Verbiest[3,4] ascribed NIC to direct mechanical compression of the nerve root, whereas Blau and Logue[5] supported an ishemic mechanism at a root level and proposed that exercise-induced vasodilation would induce an increase in the pressure in the nerve roots. On the other hand, Kavanaugh et al[6] reported the venous congestion in the cauda equina induced when the obstruction of the subarachnoid space and the increase of CSF pressure occurred by intermittent mechanical constriction. Therefore, they supported a venous mechanism as a cause of NIC. Although pathophysiology of the cauda equina induced by arterial ishchemia or venous congestion has been an object of study for a long time,[7-13] there is little agreement over which is more essential for NIC, ischemia or congestion.

MR imaging is useful because it can noninvasively reveal the severity of LSCS. Jinkins[14-16] observed abnormal nerve root enhancement at the site of stenosis on gadolinium-enhanced MR imaging in patients with LSCS and assumed that it represented the breakdown of the blood-nerve barrier at sites of nerve root injury with ensuing ascending or descending Wallerian degeneration. The basic pathology of circulatory disturbance by intermittent mechanical constriction, however, is not fully understood. Therefore, to confirm the signal intensity changes in the cauda equina observed on enhanced MR imaging pathologically, we prepared a cauda equina constriction model in dogs to test the hypothesis that the visualization of cauda equina edema is possible by gadolinium-enhanced MR images from patients with LSCS.

Received May 9, 2005; accepted after revision July 20.

From the Department of Orthopaedics and Rehabilitation Medicine (S.K., K.U., K.T., H.B.), Fukui University School of Medicine, Matsuoka, Fukui, Japan; Suzuki Orthopaedic Clinic (Y.S.), Toki, Gifu, Japan; Department of Radiology and Orthopaedics (K.H.), Aiko Orthopaedic Hospital, Midori, Aichi, Japan; and Department of Orthopaedics (H.Y.), Tachikawa Kyousai, Hospital Tachikawa, Tokyo, Japan.

Address correspondence to Shigeru Kobayashi, MD, PhD, Department of Orthopaedics and Rehabilitation Medicine, Fukui University School of Medicine, Shimoaizuki 23, Matsuoka, Fukui, 910-1193, Japan.

Methods

The experiment was carried out under the control of the local animal ethics committee in accordance with the guidelines on animal experiments in our university, Japanese government animal protection and management law, and Japanese government notification on feeding and safekeeping of animals. Nineteen adult dogs, weighing 7–15 kg, were anesthetized with intramuscular injection of 3 mL of Ketalar (Ketamine 50 mg/mL; Warner-Lambert, Morris Plains, NJ) and ventilated on a respirator under general anesthesia (O_2, 3 mL/min; N_2O, 3 mL/min; Halothane, 1.5 mL/min). Animals were maintained at constant physiologic levels during the experiment. Each animal was placed in the prone position on a frame. The sixth and seventh lumbar laminae were removed, and the dura mater was exposed widely. To confirm the signal intensity changes in the cauda equina observed on enhanced MR imaging pathologically, we applied circumferential compression outside the dura mater by using a 5-mm-long silicone tube, which caused 30% constriction of the diameter of the dura mater (average ± SEM, 18.2 ± 0.8 mm; $n = 20$; Fig 1). A digitizer with MR apparatus measured the area of the dural sac on transverse images. The cross-sectional area of control and 30%

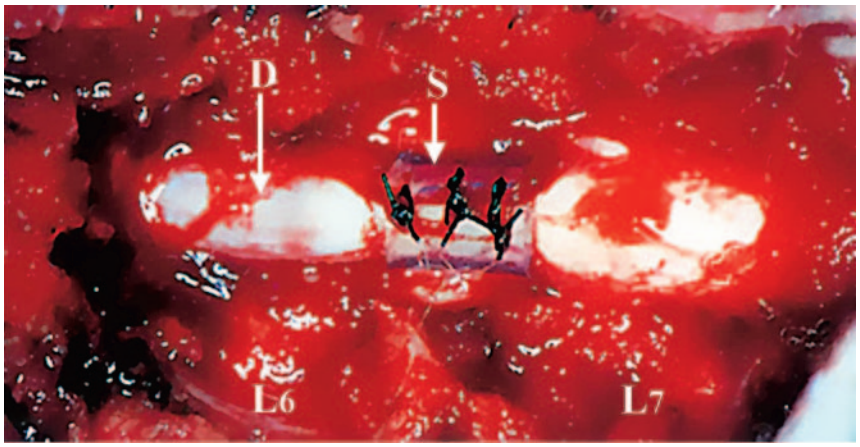

Fig 1. Circumferential compression of the cauda equina. The cauda equina was constricted outside the dura mater (D) by using a silicone tube (S), which caused 30% constriction of the diameter of the dura mater by using a silicone tube at L6/7 disk level.

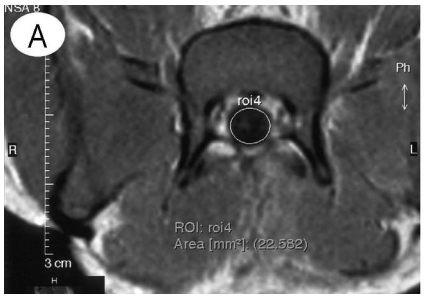

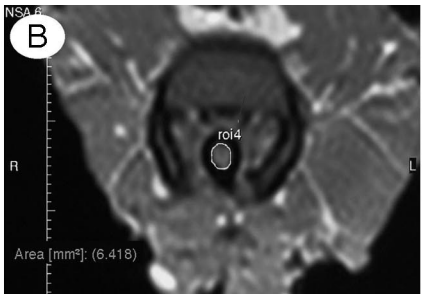

C

Cross sectional area (mm^2) of the dural sac

Subject	Control	1 week-constriction	3 weeks-constriction
1	26.0	14.1	15.3
2	22.3	15.6	14.6
3	29.1	6.4	10.2
4	21.2	13.4	8.7
5	25.9	7.4	14.0
6	28.4	14.8	14.2
7	/	15.3	7.6
average	25.5	12.4	12.1
S.E.M	3.2	3.9	3.2

Fig 2. Dural sac measurements on MR imaging. *A,* Control group. *B,* 30% constriction group. *C,* Cross-sectional area (mm^2) of the dural sac in control and 30% constriction model.

constriction model was 25.5 ± 3.2 mm^2 ($n = 6$) and 12.3 ± 3.4 mm^2 ($n = 14$), respectively (Fig 2). The cross-sectional area of 1- and 3-week constriction models were reduced 48.8% and 47.4% in comparison with control group, respectively. The incision was closed and the animal was allowed to recover. As the control group, 6 animals were evaluated at 3 weeks after laminectomy. These animals only had the dura mater exposed.

The animals were evaluated at 1 week ($n = 7$) and 3 weeks ($n = 7$) after the circumferential compression of the cauda equina. After the appropriate period of compression, the animals were sacrificed after gadolinium-diethylene-riaminepentaacetic acid (Gd-DTPA, 0.1 mmol/kg, Magnevist; Schering, Berlin Germany) and Evans blue albumin (EBA, 5 mL/kg, molecular weight approximately 59,000, Sigma Chemical Co., St. Louis) were coadministered intravenously and allowed to circulate for 30 minutes. EBA was prepared by mixing 5% bovine albumin (Wako Chemical Co) with 1% BBA (Sigma). Gd-DTPA was simultaneously injected with EBA. The cauda equina section was divided into 2 groups. At first, the changes of intraradicular vascular permeability were investigated by using MR imaging and fluorescence microscopy. In addition, the presence of intraradicular lesions was investigated by histologic and electron microscopic examination.

Preparation for Gadolinium-Enhanced Imaging

The specimens injected with Gd-DTPA and EBA were fixed by intra-aortal perfusion with 4% paraformaldehyde, and a mass of the lumbosacral spine, including the cauda equina was removed. MR studies were performed on a 0.3T permanent magnet (Magnetom; Hitachi MRP7000, Tokyo) by using 16.5-cm-diameter planar circular surface coil operating in the receive mode. A 50-cm body coil served as the transmitter. Sequences included axial T1-weighted spin-echo (SE) images, 450/25 (TR/TE), with 4-mm section thickness, 50% intersection gap, 256 × 256 matrix, and 4 excitations.[15] We compared gadolinium-enhanced MR images with EBA distribution in the nerve under a fluorescence microscope.

Preparation for Fluorescence Microscopic Study

The specimens injected with EBA were fixed in 4% paraformaldehyde for 24 hours. Twenty-micrometer-thick transverse sections of the cauda equina were mounted in 50% aqueous glycerin and examined under a fluorescence microscope at 380 mμW.[17,18] EBA emits a bright red fluorescence in clear contrast to the green fluorescence of the nerve tissue.

Preparation for Histologic and Electron Microscopic Study

The light microscopy specimens were embedded in paraffin and stained with hematoxylin-eosin (H&E) stain. The other sections were rinsed in 0.05 mol/L tris-HCl buffer, postfixed at room temperature for 3 hours in 2% OsO_4 in 0.1 mol/L sodium cacodylate buffer, impregnated with 2% uranyl acetate, dehydrated in graded ethanols, and embedded in epoxy resin. For light microscopy, 1–3-μm-thick toluidin blue–stained sections were used. For electron microscopy, ultrathin sections contrasted with uranyl acetate and lead citrate were examined a under JSM2000 electron microscope (Hitachi).[19]

Results

Changes of Intraradicular Vascular Permeability after Nerve Root Compression

The cauda equina showed low intensity on gadolinium-enhanced MR images in the control group (Fig 3*A*), and fluorescence microscopy of the cauda equina extracted after MR images revealed localization of EBA in the vessels (Fig 3*B*).

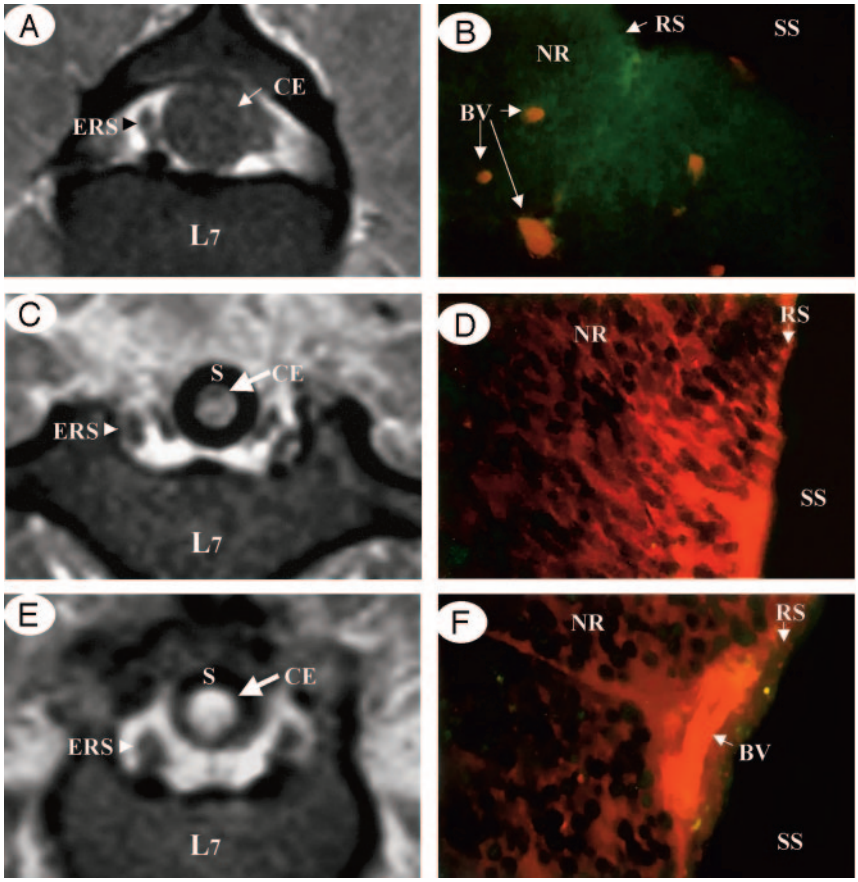

Fig 3. Comparison between enhanced MR imaging and fluorescent micrograph of the cauda equina.

A and *B,* Control group. No enhancement of a healthy cauda equina (CE) was found on a gadolinium-enhanced MR image (T1-weighted spin-echo [SE] image, 600/25 [TR/TE]). The cauda equina and epidural root sleeves (ERS) showed moderate signal intensities and the signal intensity was similar to that of muscle in normal conditions (*A),* EBA emits a bright red fluorescence in clear contrast to the green fluorescence of the nerve tissue. EBA was limited inside the blood vessels, and the blood-nerve barrier was maintained as seen under fluorescent microscopy (*B*).

C and *D,* After 1 week constriction.

E and *F,* After 3 weeks constriction. Clear enhancement was seen inside the cauda equina constricted by a silicon tube (*S*) as seen on gadolinium-enhanced MR image. No enhancement of epidural root sleeves (ERS) was found on gadolinium-enhanced MR image (T1-weighted spin-echo [SE] image, 600/25 [TR/TE]) (*C* and *E*). In the cauda equina, where enhancement was found on MR imaging, EBA emits a bright red fluorescence, which leaked outside the blood vessels, and intraradicular edema was seen under a fluorescent microscope (*D* and *F*). BV, blood vessel; CE, cauda equine; ENS, epidural root sleeves; NR, nerve root; RS, root sheath; SS, subarachnoid space.

These findings show that the blood-nerve barrier is present in each nerve root of the cauda equina. In the cauda equina constriction model, however, gadolinium-enhanced MR images demonstrated contrast enhancement of the cauda equina at the site of constriction in all animals after 1 and 3 weeks of constriction (Fig 3*C, -E*). Fluorescence microscopy also revealed extravascular leakage of EBA, and intraradicular edema was noted (Fig 3*D, -F*).

Morphologic Changes of the Nerve Roots after Mechanical Compression

One week after cauda equina constriction, histologic and electron microscopic examination of these regions showed deformation of the myelin sheath and the nerve fibers were separated (Fig 4*A, -B*). There were a large number of myelin ellipsoids and double membranes caused by folding of the myelin sheath, and the Schwann cells were swollen. In addition, macrophages phagocytizing myelin debris were seen between the separated nerve fibers. Light microscopy of the compressed site 3 weeks after constriction showed marked intraradicular nerve fiber degeneration and also revealed congestion and dilation of the intraradicular veins and Wallerian degeneration at the site of constriction (Figs 5 and 7*A*). Nerve fiber degeneration affecting the dorsal root central to the site of constriction and the ventral root peripheral to it was more advanced than after 1 week (Fig 6). Under the electron microscope, the destruction of the myelin sheath had progressed to the stage where there was little myelin formation, detachment of the basal lamina, and formation of whorls of various sizes. Accumulation of myelin debris within Schwann cells resulted in the loss of membranous structures. Furthermore, myelin droplets, fatty aggregates with a strong osmium affinity, had formed and there were large numbers of nerve fibers with a myelin sheath but no axons. Electron microscopy also revealed numerous macrophages in the perivascular space (Fig 7*B*), and macrophages capable of passing through the vessel walls were also observed. These intraradicular blood vessels revealed discontinuous capillaries with separation between the endothelial cells and breakdown of the blood-nerve barrier (Fig 7*C*). These findings were also indicative of increased vascular permeability.

No Wallerian degeneration was evident in the dorsal root peripheral to the site of compression or in the ventral root central to this site even at 3 weeks after compression. After 1 and 3 weeks, histologic examination of the control group revealed nerve fiber deformation but no appreciable Wallerian degeneration (Fig 8).

Discussion

Because surgery is the usual treatment for LSCS, it is important to clarify the differing theories as to underlying physiology of neurogenic intermittent clarification, whether it is arterial or venous ischemia, or whether it is related to restriction of CSF or is secondary to a combination of factors. Such a determination of pathophysiology may lead to improved adjunctive medial therapies and better prediction of treatment outcome.

Both the cauda equina and the nerve roots in the dural sleeve lie within the subarachnoid space and thus are suspended in CSF. The nerve root sheath is very thin and lacks a diffusion barrier corresponding to the perineurium of peripheral nerves, so the endoneurial space is continuous with the subarachnoid space.[20,21]

Accordingly, the diffusion barrier is found deeper in the arachnoid membrane at the inner wall of the dura mater and

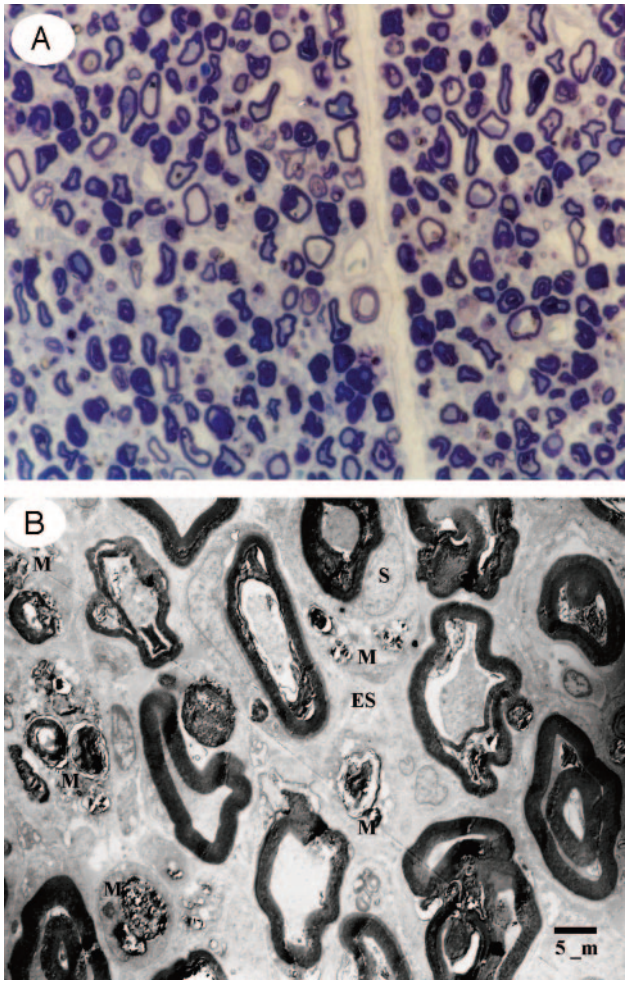

Fig 4. Light (*A*) and electron micrographs (*B*) in the cauda equina at the site of constriction after 1 week. One week after cauda equina constriction, Wallerian degeneration was apparent in the constriction area. Histologic and electron microscopic examination of these regions showed deformation of the myelin sheath and the nerve fibers were separated. In addition, macrophages phagocytizing myelin debris were seen between the separated nerve fibers. *A,* Toluidin blue stain: ×50. *B,* ×1500 (ES, endoneurial space; M, macrophage; S, Schwann cell).

the dural sleeve.[22-24] The capillary vessels of the nerve root are continuous vessels with vascular endothelial cells, which contain only a few pinocytic vesicles that are bound by tight junctions and form the blood-nerve barrier.[25] A tracer protein that is injected intravenously does not leak out of the vessels due to this barrier; however, a tracer protein injected into the subarachnoid space enters the endoneurial space of the spinal nerve root, is transferred to the capillaries by pinocytotic vesicles, and is excreted in the veins. That is, as pointed out by Kobayashi et al, the existence of a blood-nerve barrier does not necessarily mean that there is a corresponding nerve-blood barrier.[25] Because of such specific anatomic features of the cauda equina and nerve root, the mechanism involved in the development of cauda equina and radicular symptoms in patients with LSCS is somewhat different from that related to the development of peripheral nerve symptoms.

Delamarter et al[26-28] have studied the effects of prolonged compression of the cauda equina in dogs. The cauda equina was acutely constricted by 25%, 50%, or 75% of its initial circumference by using a nylon band. The constriction was maintained for 3 months. There were no or only initial neurologic deficits in the 25% constriction series. They reported that constriction of more than 50% was the critical point that resulted in complete loss of cortical evoked potentials and in neurologic deficits and histologic abnormalities. Therefore, we used the model of 30% constriction to prevent palaplesia and urinary incontinence.

The contrast enhancement of MR imaging is determined by 3 factors, including the intravascular component, the extravascular component, and the relaxation time properties of the tissues.[29,30] The capillaries of the cauda equina have the blood-nerve barrier, so Gd-DTPA does not leak out of the vessels in the normal state. In this study, Gd-DTPA does not leak out of the vessels in the normal state because the vessels in the cauda equina have a blood-nerve barrier; however, if cauda equina constriction is present due to canal stenosis, intraradicular circulatory disturbance and nerve degeneration can break down the blood-nerve barrier, causing intraradicular edema.[31,32] These findings were considered an explanation to the contrast enhancement of the cauda equina at the site of canal stenosis, namely, intraradicular edema was detected by gadolinium-enhanced MR images.

An experiment performed by Olmarker et al in 1989 demonstrated that the capillaries and venules of the nerve root could be occluded by mild compression of 30–40 mm Hg.[33]

In compression radiculopathy, total circumferential compression of the cauda equina associated with closure of the subarachnoid space is assumed to block all routes for the supply of nourishment and removal of waste via the CSF, and thereby triggering various disorders in combination with chemical factors released by inflammatory cells. Some experimental studies on changes in vascular permeability with Wallerian degeneration have focused on the peripheral nerves[34-36] and nerve roots.[32,37] Seitz et al[35] crushed the sciatic nerves of mice and used various tracers to observe vascular permeability in the endoneurium during Wallerian degeneration. In the degenerating portion of the nerve distal to the site of compression, vascular permeability peaked on day 8. As the nerve regenerated, extravasation of tracers declined and by day 30 the blood-nerve barrier was almost intact. It was suggested that increased vascular permeability was related to the greater demand for energy during neural regeneration.

Although there are no lymphatic vessels in the nervous system tissue, macrophages are present as in other tissue and these play a major role in the removal of foreign material. In the spinal cord and nerve roots within the subarachnoid space, the CSF is believed to have a role similar to that of the lymphatic circulation. The current study suggested that necrotic substances produced by Wallerian degeneration were primarily removed by macrophages originating from the mononuclear phagocytic system.[38,39] These cells are believed to have entered the nerve roots as a result of breakdown of the blood-nerve barrier. Macrophages are the chief effecter cells causing inflammatory neuritis.[40,41] Macrophages can generate a host of inflammatory molecules (eg, interleukin-1[42-44] and tumor necrosis factor [42,43,45]) and can also exert cytotoxic activity by direct physical contact or through the release of toxic byproducts (eg, nitric oxide[46] and proteases[47,48]).

Inflammatory mediators liberated from macrophages are intimately involved in the inflammatory process by enhancing

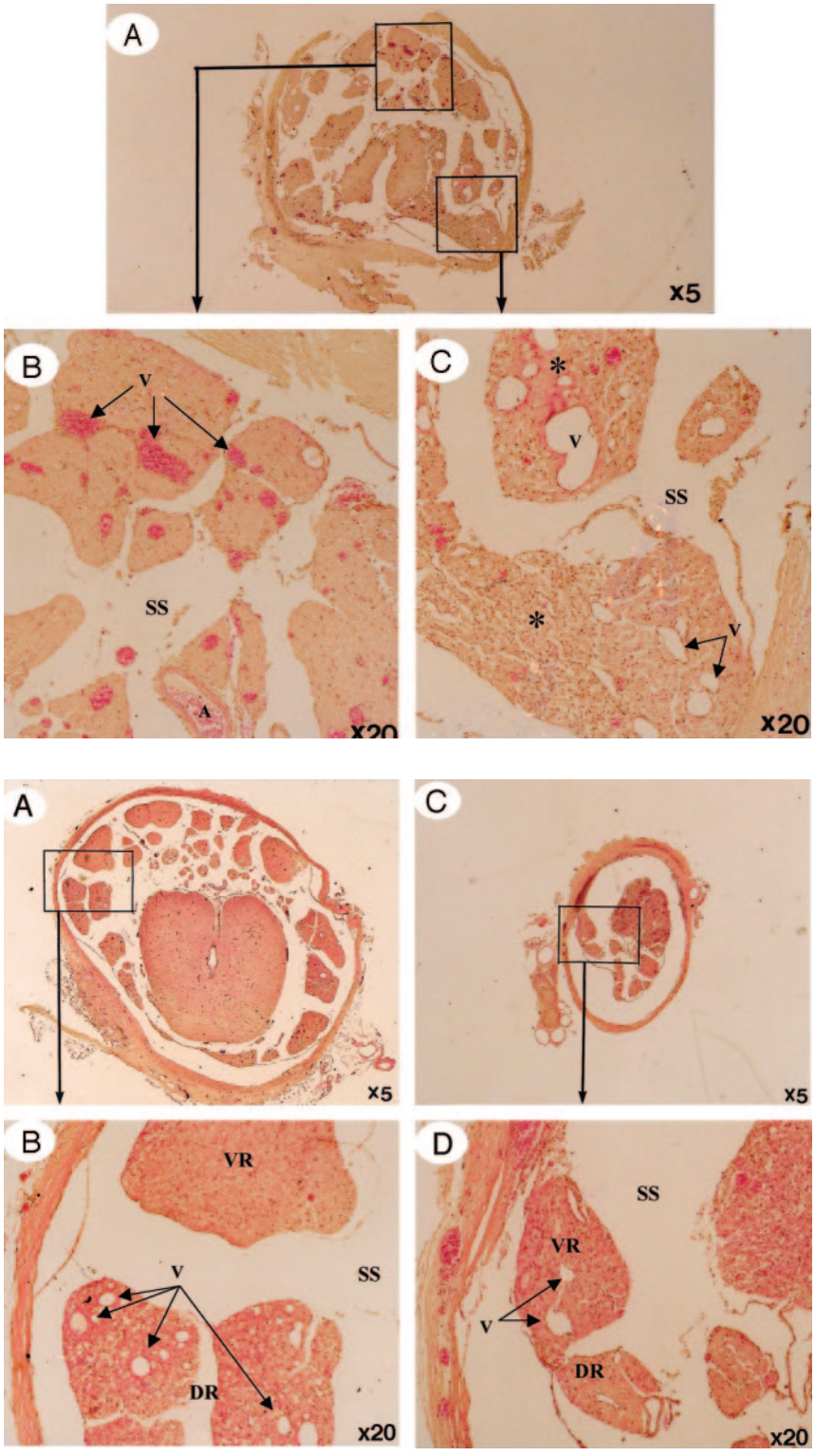

Fig 5. Light micrographs in the cauda equina at the site of constriction after 3 weeks (H&E stain).

A, A whole view of cauda equina showing as high intensity on gadolinium-enhanced MR imaging. *B,* Ventral roots. *C,* Dorsal roots. Light microscopy revealed congestion and dilation of the radicular veins (*B* and *C, arrows*) inside the cauda equina, inflammatory cell infiltration, and Wallerian degeneration (*C, asterisks*) observed in the entrapped region. This situation reflected breakdown of blood–nerve barrier on fluorescent microscopy and high intensity on gadolinium-enhanced MR imaging.

Fig 6. Light micrographs in the cauda equina central (*A* and *B*) and peripheral (*C* and *D*). to the site of compression after 3 weeks. Proximal to the constriction region, venous dilation and Wallerian degeneration were apparent in the dorsal root, but there was no nerve fiber degeneration in the ventral root (*A* and *B*). In contrast, degeneration of nerve fibers was observed in the ventral root distal to the constriction region, a change attributed to arachnoiditis resulting from Wallerian degeneration (*C* and *D*). A, artery; DR, dorsal root; SS, subarachnoid space; V, vein; VR, ventral root.

vascular permeability, providing chemotactic signals and modulating inflammatory cell activities. The present study showed that intraradicular edema and the appearance of macrophages not only occurred at the site of constriction, but also in other degenerating regions (Fig 5).[32] This phenomenon may be one cause of chemical radiculitis. In other words, breakdown of the blood-nerve barrier and the appearance of inflammatory cells both at the site of injury and in degenerating regions may play a major role in chemical radiculitis resulting from LSCS.

We think that the primary cause of NIC is a mechanical force to the cauda equina by surrounding tissues; however, it is very difficult to distinguish acute from chronic compression to the cauda equina as the cause of NIC. The nerve roots of the lumbosacral spine always move with movement of the lower extremities, and the dynamic limit is depen-

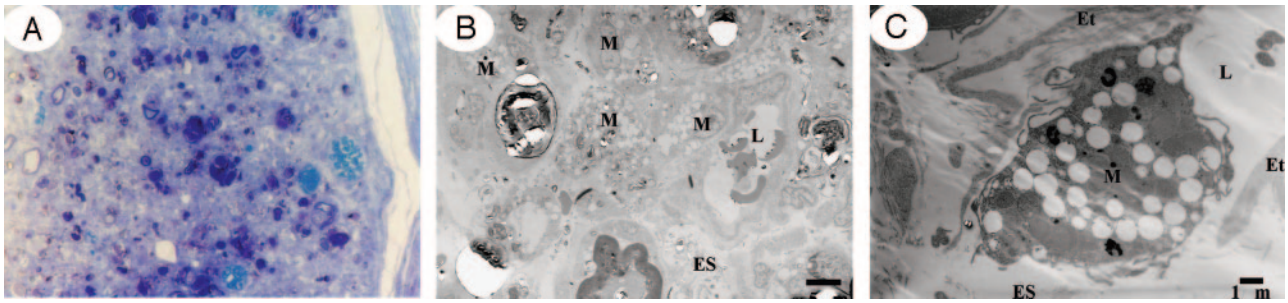

Fig 7. Light and electron micrographs in the cauda equina at the site of constriction after 3 weeks.

A, Light microscopy revealed nerve fiber degeneration. (Toluidin blue stain, ×50).

B, Electron microscopy revealed abundance of macrophages phagocytosing the degenerated myelin sheath (×1500).

C, High magnification of a capillary revealed separation of the tight junction to allow communication between the vascular lumen and endoneurial space, indicating breakdown of the blood-nerve barrier and a macrophage capable of passing through the vessel walls (×5000).

dent on the positional relationship between the cauda equina and the surrounding tissues. Thus, when narrowing of the spinal canal is caused by surrounding tissues, movement of the cauda equina along with movement of the lower extremities becomes limited, and consequently compression and traction on the cauda equina cause the disturbance of intraradicular blood flow. Chronic compression is the result of repeated episodes of mild acute compression. Our clinical experience has shown that NIC is frequently alleviated by rest in patients with LSCS and is intensified by application of acute compression to the cauda equina during walking.

In the present study, the increase of vascular permeability in the cauda equina after compression was more marked at 1 week than at 3 weeks. Histologic studies in the circumferential constriction model of the cauda equina also revealed congestion and dilation of the intraradicular veins and Wallerian degeneration at the site of constriction.

These changes were considered to be attributed to intraradicular edema and were thought to explain the enhancement effect at the site of canal stenosis on gadolinium-enhanced MR images in LSCS patients (Fig 9). These results suggest that intermittent claudication in LSCS is caused by the following mechanism. Stenosis of the lumbar canal is aggravated by posterior flexion during walking, and circumferential mechanical compression of the cauda equina occurs repeatedly and increases in severity.

As a result, the subarachnoid space is occluded, and congestion, as well as degeneration of nerve fibers, occurs in the cauda equina. Efflux of excess fluid into the subarachnoid space becomes impaired by the breakdown of the blood-nerve barrier, leading to an increase in endoneurial pressure.[49,50] Although such a pressure rise is reversible, a compartment syndrome may occur in the cauda equina at the site of stenosis, blood flow,[51,52] and axonal flow disturbance,[53,54] provoking ectopic discharge or conduction disturbance[55,56] that is essentially responsible for NIC in nerve fibers which have been chronically damaged.

Conclusion

Inflammatory reaction—such as breakdown of blood-nerve barrier, Wallerian degeneration, and appearance of macrophages—may be involved in radiculitis arising from circumferential compression of the cauda equina, and these factors seem to be important in the manifestation of radiculopathy and NIC. The affected cauda equina was strongly enhanced with Gd-DTPA, indicating a blood-nerve barrier breakdown in the affected nerve root with production of intraradicular edema. That is, the ability of Gd-DTPA to contrast-enhance selectively a pathologic focus within the cauda equina is perhaps its most important clinical application and gadolinium-enhanced MR imaging might have

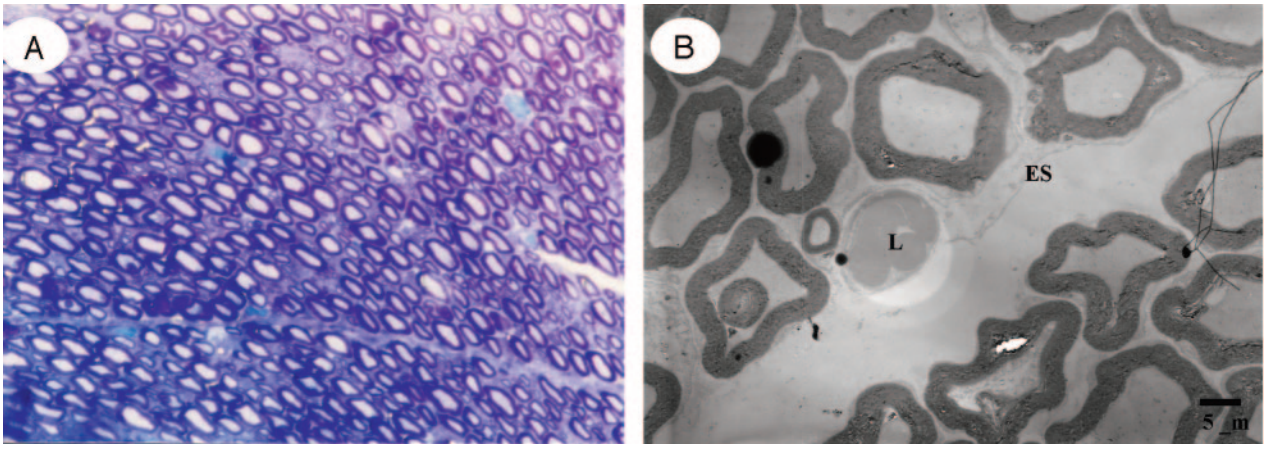

Fig 8. Light (*A*) and electron (*B*) micrographs in the cauda equina of control group. After 3 weeks, no Wallerian degeneration was evident in the nerve root.

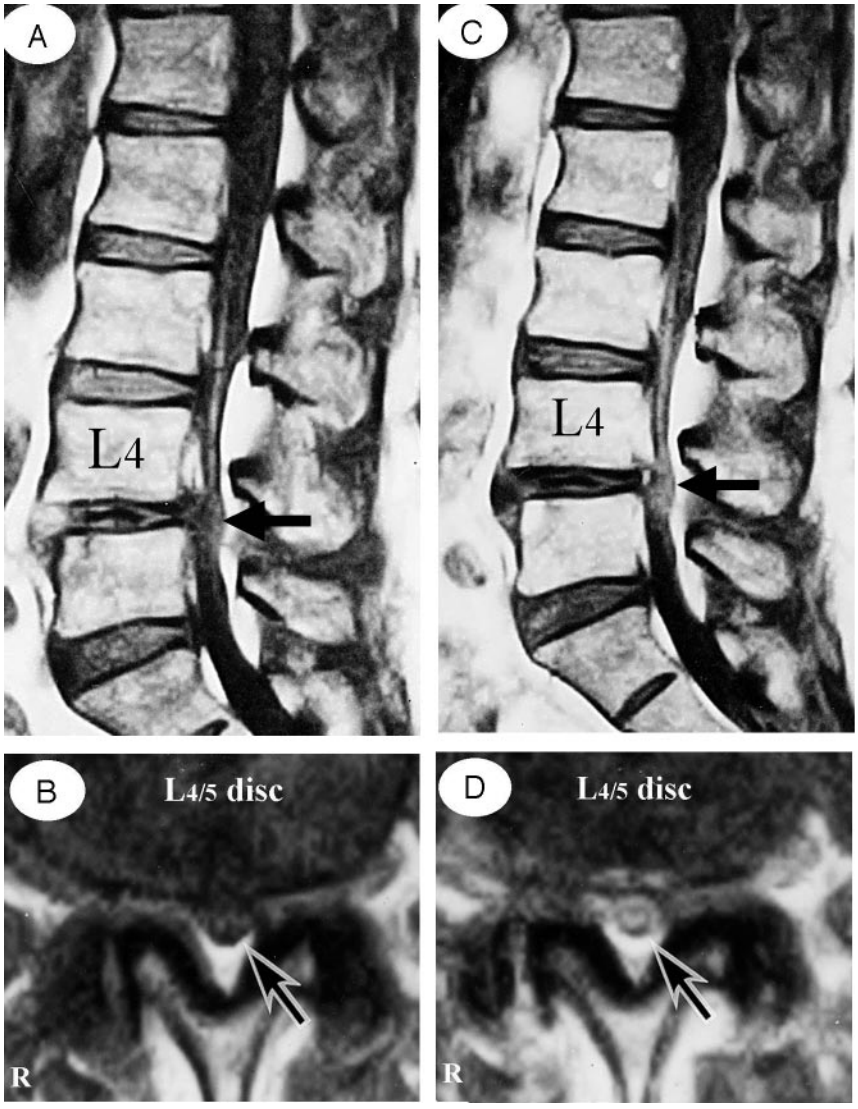

Fig 9. A 73-year-old man complained of weakness and numbness of the lower extremities after walking about 300 meters, but no obvious sensory loss and muscle weakness were noted. *A* and *B,* Precontrast T1-weighted (500/35) sagittal (*A*) and axial (*B*) conventional spin-echo MR images indicated a diagnosis of LSCS at L4/5 disk level (*arrows*). *C* and *D,* T1-weighted (500/35) sagittal (*C*) and axial (*D*) MR images acquired at L4/5 disk level obtained after 0.1 mmol/kg intravenous Gd-DTPA administration showing the generalized central canal stenosis as well as punctuate areas of intrathecal enhancement (*arrows*), which indicates a breakdown in the blood-nerve barrier.

the advantage of deciding on the range of cauda equina decompression in patients with NIC and LSCS.

Acknowledgments

The submitted manuscript does not contain information about medical devices or drugs. No benefits in any form have been received or will be received from a commercial party related directly or indirectly to the subject of this article. Mr. Takashi Nakane provided expert help with the MR imaging study. Mr. Naruo Yamashita provided expert help with the photography. The authors would like to thank Ms. Mika Osaki and Ms. Yukiko Horiuchi for their dedicated assistance in this study.

References

1. Martinelli TA, Wiesel SW. **Epidemiology of spinal stenosis.** *Instr Course Lect* 1992;41:179–81
2. Johnsson KE. **Lumbar canal stenosis: a retrospective study of 163 cases in southen Sweden.** *Acta Orthop Scand* 1995;66:403–405
3. Verbiest H. **A radicular syndrome from developmental narrowing of the lumbar vertebral canal.** *J Bone Joint Surg* 1954;36B:230–37
4. Verbiest H. **Further experiences on the pathological influence of a developmental narrowness of the bony lumbar vertebral canal.** *J Bone Joint Surg* 1955; 37B:576–83
5. Blau JN, Logue V. **Intermittent claudication of the cauda equine: an usual syndrome resulting from central protrusion of a lumbar intervertebral disc.** *Lancet* 1961;1:1081–86
6. Kavanaugh GJ, Svien HJ, Holman CB, et al. **"Pseudoclaudication" syndrome produced by compression of cauda equina.** *JAMA* 1968;206: 2477–81
7. Crock HV, Yoshizawa H. *The blood supply of the vertebral column and spinal cord in man.* New York: Springer-Verlag;1977
8. Parke WW, Gammell K, Rothman RH. **Arterial vascularization of the cauda equina.** *J Bone Joint Surg [Am]* 1981;63:53–62
9. Parke WW, Watanabe R. **The intrinsic vasculature of the lumbosacral spinal nerve roots.** *Spine* 1985;10:508–15
10. Crock HV, Yamagishi M, Crock MC. *The conus medullaris and cauda equina in man.* New York: Springer-Verlag;1986
11. Watanabe R, Parke WW. **Vascular and neuralpathology of lumbosacral spinal stenosis.** *J Neurosurg* 1986;64:64–70
12. Kobayashi S, Yoshizawa H, Nakai S. **Experimental study on the dynamics of lumbar nerve root circulation.** *Spine* 2000;25:298–305
13. Parke WW. **The significance of impaired venous return in ishchemic radiculopathy and myelopathy.** *Orthop Clin North Am* 1991;22:213–21
14. Jinkins R. **Gd-DTPA enhanced MR of the lumbar spinal canal in patients with claudication.** *J Comput Assist Tomogr* 1993;17:555–62
15. Jinkins R. **MR of enhancing nerve roots in the unoperated lumbosacral spine.** *AJNR Am J Neuroradiol* 1993;14:193–202
16. Jinkins R. **Magnetic resonance imaging of benign nerve root enhancement in the unoperated and postoperative lumbosacral spine.** *Neuroimag Clin N Am* 1993;3:525–41
17. Kobayashi S, Meir A, Baba H, et al. **Imaging of intraneural edema using gadolinium-enhanced MR imaging: experimental compression injury.** *AJNR Am J Neuroradiol* 2005;26:973–80
18. Kobayashi S, Yoshizawa H. **Effect of mechanical compression on the vascular permeability of the dorsal root ganglion.** *J Orthop Res* 2002;20:730–39
19. Kobayashi S, Yoshizawa H, Yamada S. **Pathology of lumbar nerve root compression. Part 2. Morphological and immunohistochemical changes of dorsal root ganglion.** *J Orthop Res* 2004;22:180–88
20. Gamble HJ. **Comparative electron microscopic observations on the connective tissues of a peripheral nerve and a spinal nerve root in the rat.** *J Anat (London)* 1964;98:17–25
21. Haller FR, Low FN. **The fine structure of the peripheral nerve root sheath in the subarachnoid space in the rat and other laboratory animals.** *Am J Anat* 1971;131:1–20
22. Haller FR, Haller FC, Low FN. **The fine structure of cellular layers and connective tissue space at spinal nerve root attachments in the rat.** *Am J Anat* 1972; 133:109–24
23. Yoshizawa H, Kobayashi S, Hachiya Y. **Blood supply of nerve roots and dorsal root ganglia.** *Orthop Clin North Am* 1991;22:195–211
24. Yoshizawa H., Kobayashi S., Kubota K. **Effect of compression on intraradicular blood flow in dogs.** *Spine* 1989;14:1220–25
25. Kobayashi S, Yoshizawa H, Hachiya Y, et al. **Vasogenic edema induced by intravenously injected protein tracers and gadolinium-enhanced magnetic resonance imaging.** *Spine* 1993;18:1410–24
26. Delamarter RB, Bohlman HH, Dodge LD, et al. **Experimantal lumbar spinal stenosis.** *J Bone Joint Surg* 1990;72A:110–20

27. Delamarter RB, Bohlman HH, Bodner D, et al. **Urologic function after experimental cauda equina compression: cystometrograms versus cortical-evoked potentials.** *Spine* 1990;15:864–70
28. Delamarter RB, Sherman JE, Carr JB, et al. **1991 Volvo Award in Experimental Studies: cauda equina syndrome: neurologic recovery following immediate, early or late decompression.** *Spine* 1991;16:1022–29
29. Gado MH, Phelps ME, Coleman RE. **A extravascular component of contrast enhancement in cranial tomography. Part I. Tissue-blood ratio of contrast enhancement.** *Radiology* 1975;117:589–93
30. Gado MH, Phelps ME, Coleman RE. **A extravascular component of contrast enhancement in cranial tomography. Part II. Contrast enhancement and blood-tissue barrier.** *Radiology* 1975;117:595–97
31. Yoshizawa H., Kobayashi S., Morita T. **Chronic nerve root compression: pathophysiologic mechanism of nerve root dysfunction.** *Spine* 1995;20:397–407
32. Kobayashi S, Yoshizawa H, Yamada S. **Pathology of lumbar nerve root compression. Part 1. Intraradicular inflammatory changes induced by mechanical compression.** *J Orthop Res* 2004;22:170–79
33. Olmarker K, Rydevik B, Holm S. **Effect of experimental, graded compression on blood flow in spinal nerve roots: a vital microscopic study on the porcine cauda equina.** *J Orthop Res* 1989;7:817–23
34. Mellick RS, Cavanagh JB. **Changes in blood vessel permeability during degeneration and regeneration in peripheral nerves.** *Brain* 1967;91:141–60
35. Seitz RJ, Reiners K, Himmelmann F, et al. **The blood-nerve barrier in Wallerian degeneration: a sequential long-term study.** *Muscle Nerve* 1989;12:627–35
36. Sparrow JR, Kiernan JA. **Endoneurial vascular permeability in degenerating and regenerating peripheral nerves.** *Acta Neuropathol (Berl)* 1981;53:181–88
37. Matsui T, Takahashi K, Moriya M, et al. **Quantitative analysis of edema in the dorsal nerve roots induced by acute mechanical compression.** *Spine* 1998;23:1931–36
38. Van Furth R, Cohn ZA. **The origin and kinetics of mononuclear phagocytes.** *J Exp Med* 1968;128:415–33
39. Van Furth R, Cohn ZA, Hirsch JG, et al. **The mononuclear phagocyte system: a new classification of macrophages, monocytes and their precursor cells.** *Bull Wld Hlth Org* 1972;46:845–52
40. Kobayashi S, Baba H, Uchida K, et al. **Effect of mechanical compression on the lumbar nerve root: localization and changes of intraradicular inflammatory cytokines, nitric oxide, and cyclooxygenase.** *Spine* 2005;30:1699–705
41. Kobayashi S, Baba H, Uchida K, et al. **Localization and changes of intraneural inflammatory cytokines and inducible-nitric oxide induced by mechanical compression.** *J Orthop Res* 2005;23:771–8
42. DeLeo JA, Colburn RW. **The role of cytokines in nociception and chronic pain**. In: Weinstein J, ed. *Low back pain: a scientific and clinical overview. Am Acad Orthpaed Surg* 1977;163–85
43. Dinarello CA. **The biology of interleukin 1 and comparison to tumor necrosis factor.** *Immunol Lett* 1987;16:227–30
44. Rotshenker S, Aamar S, Barak V. **Interleukin-1 activity in lesioned peripheral nerve.** *J Neuroimmunol* 1992;39:75–80
45. Beutler B, Greenwald D, Hulmes JD, et al. **Identify of tumor necrosis factor and the macrophage-secreted factor cachectin.** *Nature* 1985;316:552–54
46. Moncada S, Palmer RMJ, Higgs EA. **Nitric oxide: physiology, pathophysiology, and pharmacology.** *Pharmacol Rev* 1991;43:109–42
47. Dayer JM, Russell RGG, Krane SM. **Collagenase production by rhematoid synovial cells: stimulation by a human lymphocyte factor.** *Science* 1977;195:181–83
48. Murphy G, Nagase H, Brinckerhoff CE. **Relationship of procollagenase activator, stromelysin and matrix metalloproteinase 3.** *Collagen Rel Res* 1988;8:389–95
49. Rydevik B., Myers RR, Powell HC. **Pressure increase in dorsal root ganglion following mechanical compression: closed compartment syndrome in nerve roots.** *Spine* 1989;14:574–76
50. Myers RR. **The neuropathology of nerve injury and pain.** In: Weinstein J, ed. *Low back pain: a scientific and clinical overview. Am Acad Orthpaed Surg* 1997;247–64
51. Kobayashi S, Shizu N, Suzuki Y, et al. **Changes of nerve root motion and intraradicular blood flow during an intraoperative SLR test.** *Spine* 2003;28:1427–34
52. Kobayashi S, Suzuki Y, Asai T, et al. **Changes of nerve root motion and intraradicular blood flow during an intraoperative femoral nerve stretch test.** *J Neurosurg (Spine 3)* 2003;99:298–305
53. Kobayashi S, Kokubo Y, Uchida K, et al. **Effect of lumbar nerve root compression on primary sensory neurons and their central branches: changes in the nociceptive neuropeptides substance P and somatostatin.** *Spine* 2005;30:276–82
54. Kobayashi S, Sasaki S, Shimada S, et al. **Changes of carcitonin gene-related peptide in primarily sensory neuron and their central branch after nerve root compression of the dog.** *Arch Phys Med Rehabil* 2005;86:527–33
55. Howe JF, Loser JD, Calvin WH. **Mechanosensitivity of dorsal root ganglia and chronically injured axons: a physiological basis for the radicular pain of nerve root compression.** *Pain* 1977;3:25–41
56. Calvin WH. **Some design features of axons and how neuralgias may defeat them: advances in pain research and therapy.** *Pain* 1979;3:297–309